Editor's Focus

Search for the doubly charmed baryon Ξ_{cc}^+

LHCb Collaboration

R. Aaij[31], C. Abellán Beteta[49], T. Ackernley[59], B. Adeva[45], M. Adinolfi[53], H. Afsharnia[9],
C. A. Aidala[79], S. Aiola[25], Z. Ajaltouni[9], S. Akar[64], P. Albicocco[22], J. Albrecht[14], F. Alessio[47],
M. Alexander[58], A. Alfonso Albero[44], G. Alkhazov[37], P. Alvarez Cartelle[60], A. A. Alves Jr[45],
S. Amato[2], Y. Amhis[11], L. An[21], L. Anderlini[21], G. Andreassi[48], M. Andreotti[20], F. Archilli[16],
J. Arnau Romeu[10], A. Artamonov[43], M. Artuso[67], K. Arzymatov[41], E. Aslanides[10], M. Atzeni[49],
B. Audurier[26], S. Bachmann[16], J. J. Back[55], S. Baker[60], V. Balagura[11,b], W. Baldini[20,47], A. Baranov[41],
R. J. Barlow[61], S. Barsuk[11], W. Barter[60], M. Bartolini[23,47,h], F. Baryshnikov[76], G. Bassi[28],
V. Batozskaya[35], B. Batsukh[67], A. Battig[14], V. Battista[48], A. Bay[48], M. Becker[14], F. Bedeschi[28],
I. Bediaga[1], A. Beiter[67], L. J. Bel[31], V. Belavin[41], S. Belin[26], N. Beliy[5], V. Bellee[48], K. Belous[43],
I. Belyaev[38], G. Bencivenni[22], E. Ben-Haim[12], S. Benson[31], S. Beranek[13], A. Berezhnoy[39],
R. Bernet[49], D. Berninghoff[16], H. C. Bernstein[67], E. Bertholet[12], A. Bertolin[27], C. Betancourt[49],
F. Betti[19,e], M. O. Bettler[54], Ia. Bezshyiko[49], S. Bhasin[53], J. Bhom[33], M. S. Bieker[14], S. Bifani[52],
P. Billoir[12], A. Birnkraut[14], A. Bizzeti[21,u], M. Bjørn[62], M. P. Blago[47], T. Blake[55], F. Blanc[48], S. Blusk[67],
D. Bobulska[58], V. Bocci[30], O. Boente Garcia[45], T. Boettcher[63], A. Boldyrev[77], A. Bondar[42,x],
N. Bondar[37], S. Borghi[61,47], M. Borisyak[41], M. Borsato[16], J. T. Borsuk[33], T. J. V. Bowcock[59],
C. Bozzi[20,47], S. Braun[16], A. Brea Rodriguez[45], M. Brodski[47], J. Brodzicka[33], A. Brossa Gonzalo[55],
D. Brundu[26], E. Buchanan[53], A. Buonaura[49], C. Burr[47], A. Bursche[26], J. S. Butter[31], J. Buytaert[47],
W. Byczynski[47], S. Cadeddu[26], H. Cai[71], R. Calabrese[20,g], S. Cali[22], R. Calladine[52], M. Calvi[24,i],
M. Calvo Gomez[44,m], A. Camboni[44,m], P. Campana[22], D. H. Campora Perez[47], L. Capriotti[19,e],
A. Carbone[19,e], G. Carboni[29], R. Cardinale[23,h], A. Cardini[26], P. Carniti[24,i], K. Carvalho Akiba[31],
A. Casais Vidal[45], G. Casse[59], M. Cattaneo[47], G. Cavallero[47], R. Cenci[28,p], J. Cerasoli[10],
M. G. Chapman[53], M. Charles[12,47], Ph. Charpentier[47], G. Chatzikonstantinidis[52], M. Chefdeville[8],
V. Chekalina[41], C. Chen[3], S. Chen[26], A. Chernov[33], S.-G. Chitic[47], V. Chobanova[45], M. Chrzaszcz[47],
A. Chubykin[37], P. Ciambrone[22], M. F. Cicala[55], X. Cid Vidal[45], G. Ciezarek[47], F. Cindolo[19],
P. E. L. Clarke[57], M. Clemencic[47], H. V. Cliff[54], J. Closier[47], J. L. Cobbledick[61], V. Coco[47],

J. A. B. Coelho[11], J. Cogan[10], E. Cogneras[9], L. Cojocariu[36], P. Collins[47], T. Colombo[47],

A. Comerma-Montells[16], A. Contu[26], N. Cooke[52], G. Coombs[58], S. Coquereau[44], G. Corti[47],

C. M. Costa Sobral[55], B. Couturier[47], D. C. Craik[63], J. Crkovska[66], A. Crocombe[55], M. Cruz Torres[1],

R. Currie[57], C. L. Da Silva[66], E. Dall'Occo[31], J. Dalseno[45,53], C. D'Ambrosio[47], A. Danilina[38],

P. d'Argent[16], A. Davis[61], O. De Aguiar Francisco[47], K. De Bruyn[47], S. De Capua[61], M. De Cian[48],

J. M. De Miranda[1], L. De Paula[2], M. De Serio[18,d], P. De Simone[22], J. A. de Vries[31], C. T. Dean[66],

W. Dean[79], D. Decamp[8], L. Del Buono[12], B. Delaney[54], H.-P. Dembinski[15], M. Demmer[14],

A. Dendek[34], V. Denysenko[49], D. Derkach[77], O. Deschamps[9], F. Desse[11], F. Dettori[26], B. Dey[7],

A. Di Canto[47], P. Di Nezza[22], S. Didenko[76], H. Dijkstra[47], F. Dordei[26], M. Dorigo[28,y],

A. C. dos Reis[1], L. Douglas[58], A. Dovbnya[50], K. Dreimanis[59], M. W. Dudek[33], L. Dufour[47],

G. Dujany[12], P. Durante[47], J. M. Durham[66], D. Dutta[61], R. Dzhelyadin[43†], M. Dziewiecki[16],

A. Dziurda[33], A. Dzyuba[37], S. Easo[56], U. Egede[60], V. Egorychev[38], S. Eidelman[42,x], S. Eisenhardt[57],

R. Ekelhof[14], S. Ek-In[48], L. Eklund[58], S. Ely[67], A. Ene[36], S. Escher[13], S. Esen[31], T. Evans[47],

A. Falabella[19], J. Fan[3], N. Farley[52], S. Farry[59], D. Fazzini[11], M. Féo[47], P. Fernandez Declara[47],

A. Fernandez Prieto[45], F. Ferrari[19,e], L. Ferreira Lopes[48], F. Ferreira Rodrigues[2], S. Ferreres Sole[31],

M. Ferrillo[49], M. Ferro-Luzzi[47], S. Filippov[40], R. A. Fini[18], M. Fiorini[20,g], M. Firlej[34], K. M. Fischer[62],

C. Fitzpatrick[47], T. Fiutowski[34], F. Fleuret[11,b], M. Fontana[47], F. Fontanelli[23,h], R. Forty[47],

V. Franco Lima[59], M. Franco Sevilla[65], M. Frank[47], C. Frei[47], D. A. Friday[58], J. Fu[25,q], M. Fuehring[14],

W. Funk[47], E. Gabriel[57], A. Gallas Torreira[45], D. Galli[19,e], S. Gallorini[27], S. Gambetta[57], Y. Gan[3],

M. Gandelman[2], P. Gandini[25], Y. Gao[4], L. M. Garcia Martin[46], J. García Pardiñas[49],

B. Garcia Plana[45], F. A. Garcia Rosales[11], J. Garra Tico[54], L. Garrido[44], D. Gascon[44], C. Gaspar[47],

D. Gerick[16], E. Gersabeck[61], M. Gersabeck[61], T. Gershon[55], D. Gerstel[10], Ph. Ghez[8], V. Gibson[54],

A. Gioventù[45], O. G. Girard[48], P. Gironella Gironell[44], L. Giubega[36], C. Giugliano[20], K. Gizdov[57],

V. V. Gligorov[12], C. Göbel[69], D. Golubkov[38], A. Golutvin[60,76], A. Gomes[1,a], P. Gorbounov[38,6],

I. V. Gorelov[39], C. Gotti[24,i], E. Govorkova[31], J. P. Grabowski[16], R. Graciani Diaz[44], T. Grammatico[12],

L. A. Granado Cardoso[47], E. Graugés[44], E. Graverini[48], G. Graziani[21], A. Grecu[36], R. Greim[31],

P. Griffith[20], L. Grillo[61], L. Gruber[47], B. R. Gruberg Cazon[62], C. Gu[3], E. Gushchin[40], A. Guth[13],

Yu. Guz[43,47], T. Gys[47], T. Hadavizadeh[62], G. Haefeli[48], C. Haen[47], S. C. Haines[54], P. M. Hamilton[65],

Q. Han[7], X. Han[16], T. H. Hancock[62], S. Hansmann-Menzemer[16], N. Harnew[62], T. Harrison[59], R. Hart[31],

C. Hasse[47], M. Hatch[47], J. He[5*], M. Hecker[60], K. Heijhoff[31], K. Heinicke[14], A. Heister[14],

A. M. Hennequin[47], K. Hennessy[59], L. Henry[46], J. Heuel[13], A. Hicheur[68], R. Hidalgo Charman[61],

D. Hill[62], M. Hilton[61], P. H. Hopchev[48], J. Hu[16], W. Hu[7], W. Huang[5], Z. C. Huard[64], W. Hulsbergen[31],

T. Humair[60], R. J. Hunter[55], M. Hushchyn[77], D. Hutchcroft[59], D. Hynds[31], P. Ibis[14], M. Idzik[34], P. Ilten[52],

A. Inglessi[37], A. Inyakin[43], K. Ivshin[37], R. Jacobsson[47], S. Jakobsen[47], J. Jalocha[62], E. Jans[31],

B. K. Jashal[46], A. Jawahery[65], V. Jevtic[14], F. Jiang[3], M. John[62], D. Johnson[47], C. R. Jones[54], B. Jost[47],

N. Jurik[62], S. Kandybei[50], M. Karacson[47], J. M. Kariuki[53], N. Kazeev[77], M. Kecke[16], F. Keizer[54],

M. Kelsey[67], M. Kenzie[54], T. Ketel[32], B. Khanji[47], A. Kharisova[78], K. E. Kim[67], T. Kirn[13],

V. S. Kirsebom[48], S. Klaver[22], K. Klimaszewski[35], S. Koliiev[51], A. Kondybayeva[76],

A. Konoplyannikov[38], P. Kopciewicz[34], R. Kopecna[16], P. Koppenburg[31], I. Kostiuk[31,51], O. Kot[51], S. Kotriakhova[37], L. Kravchuk[40], R. D. Krawczyk[47], M. Kreps[55], F. Kress[60], S. Kretzschmar[13], P. Krokovny[42,x], W. Krupa[34], W. Krzemien[35], W. Kucewicz[33,l], M. Kucharczyk[33], V. Kudryavtsev[42,x], H. S. Kuindersma[31], G. J. Kunde[66], A. K. Kuonen[48], T. Kvaratskheliya[38], D. Lacarrere[47], G. Lafferty[61], A. Lai[26], D. Lancierini[49], J. J. Lane[61], G. Lanfranchi[22], C. Langenbruch[13], T. Latham[55], F. Lazzari[28,v], C. Lazzeroni[52], R. Le Gac[10], R. Lefèvre[9], A. Leflat[39], F. Lemaitre[47], O. Leroy[10], T. Lesiak[33], B. Leverington[16], H. Li[70], P.-R. Li[5,ab], X. Li[66], Y. Li[6], Z. Li[67], X. Liang[67], R. Lindner[47], F. Lionetto[49], V. Lisovskyi[11], G. Liu[70], X. Liu[3], D. Loh[55], A. Loi[26], J. Lomba Castro[45], I. Longstaff[58], J. H. Lopes[2], G. Loustau[49], G. H. Lovell[54], Y. Lu[6], D. Lucchesi[27,o], M. Lucio Martinez[31], Y. Luo[3], A. Lupato[27], E. Luppi[20,g], O. Lupton[55], A. Lusiani[28], X. Lyu[5], S. Maccolini[19,e], F. Machefert[11], F. Maciuc[36], V. Macko[48], P. Mackowiak[14], S. Maddrell-Mander[53], L. R. Madhan Mohan[53], O. Maev[37,47], A. Maevskiy[77], K. Maguire[61], D. Maisuzenko[37], M. W. Majewski[34], S. Malde[62], B. Malecki[47], A. Malinin[75], T. Maltsev[42,x], H. Malygina[16], G. Manca[26,f], G. Mancinelli[10], R. Manera Escalero[44], D. Manuzzi[19,e], D. Marangotto[25,q], J. Maratas[9,w], J. F. Marchand[8], U. Marconi[19], S. Mariani[21], C. Marin Benito[11], M. Marinangeli[48], P. Marino[48], J. Marks[16], P. J. Marshall[59], G. Martellotti[30], L. Martinazzoli[47], M. Martinelli[47,24,i], D. Martinez Santos[45], F. Martinez Vidal[46], A. Massafferri[1], M. Materok[13], R. Matev[47], A. Mathad[49], Z. Mathe[47], V. Matiunin[38], C. Matteuzzi[24], K. R. Mattioli[79], A. Mauri[49], E. Maurice[11,b], M. McCann[60,47], L. Mcconnell[17], A. McNab[61], R. McNulty[17], J. V. Mead[59], B. Meadows[64], C. Meaux[10], N. Meinert[73], D. Melnychuk[35], S. Meloni[24,i], M. Merk[31], A. Merli[25], D. A. Milanes[72], E. Millard[55], M.-N. Minard[8], O. Mineev[38], L. Minzoni[20,g], S. E. Mitchell[57], B. Mitreska[61], D. S. Mitzel[47], A. Mödden[14], A. Mogini[12], R. D. Moise[60], T. Mombächer[14], I. A. Monroy[72], S. Monteil[9], M. Morandin[27], G. Morello[22], M. J. Morello[28,t], J. Moron[34], A. B. Morris[10], A. G. Morris[55], R. Mountain[67], H. Mu[3], F. Muheim[57], M. Mukherjee[7], M. Mulder[31], D. Müller[47], J. Müller[14], K. Müller[49], V. Müller[14], C. H. Murphy[62], D. Murray[61], P. Muzzetto[26], P. Naik[53], T. Nakada[48], R. Nandakumar[56], A. Nandi[62], T. Nanut[48], I. Nasteva[2], M. Needham[57], N. Neri[25,q], S. Neubert[16], N. Neufeld[47], R. Newcombe[60], T. D. Nguyen[48], C. Nguyen-Mau[48,n], E. M. Niel[11], S. Nieswand[13], N. Nikitin[39], N. S. Nolte[47], A. Oblakowska-Mucha[34], V. Obraztsov[43], S. Ogilvy[58], D. P. O'Hanlon[19], R. Oldeman[26,f], C. J. G. Onderwater[74], J. D. Osborn[79], A. Ossowska[33], J. M. Otalora Goicochea[2], T. Ovsiannikova[38], P. Owen[49], A. Oyanguren[46], P. R. Pais[48], T. Pajero[28,t], A. Palano[18], M. Palutan[22], G. Panshin[78], A. Papanestis[56], M. Pappagallo[57], L. L. Pappalardo[20,g], W. Parker[65], C. Parkes[61,47], G. Passaleva[21,47], A. Pastore[18], M. Patel[60], C. Patrignani[19,e], A. Pearce[47], A. Pellegrino[31], G. Penso[30], M. Pepe Altarelli[47], S. Perazzini[19], D. Pereima[38], P. Perret[9], L. Pescatore[48], K. Petridis[53], A. Petrolini[23,h], A. Petrov[75], S. Petrucci[57], M. Petruzzo[25,q], B. Pietrzyk[8], G. Pietrzyk[48], M. Pikies[33], M. Pili[62], D. Pinci[30], J. Pinzino[47], F. Pisani[47], A. Piucci[16], V. Placinta[36], S. Playfer[57], J. Plews[52], M. Plo Casasus[45], F. Polci[12], M. Poli Lener[22], M. Poliakova[67], A. Poluektov[10], N. Polukhina[76,c], I. Polyakov[67], E. Polycarpo[2], G. J. Pomery[53], S. Ponce[47], A. Popov[43], D. Popov[52], S. Poslavskii[43], K. Prasanth[33], L. Promberger[47], C. Prouve[45], V. Pugatch[51], A. Puig Navarro[49], H. Pullen[62], G. Punzi[28,p], W. Qian[5], J. Qin[5], R. Quagliani[12], B. Quintana[9], N. V. Raab[17], B. Rachwal[34],

J. H. Rademacker[53], M. Rama[28], M. Ramos Pernas[45], M. S. Rangel[2], F. Ratnikov[41,77], G. Raven[32],

M. Ravonel Salzgeber[47], M. Reboud[8], F. Redi[48], S. Reichert[14], F. Reiss[12], C. Remon Alepuz[46], Z. Ren[3],

V. Renaudin[62], S. Ricciardi[56], S. Richards[53], K. Rinnert[59], P. Robbe[11], A. Robert[12], A. B. Rodrigues[48],

E. Rodrigues[64], J. A. Rodriguez Lopez[72], M. Roehrken[47], S. Roiser[47], A. Rollings[62], V. Romanovskiy[43],

M. Romero Lamas[45], A. Romero Vidal[45], J. D. Roth[79], M. Rotondo[22], M. S. Rudolph[67], T. Ruf[47],

J. Ruiz Vidal[46], J. Ryzka[34], J. J. Saborido Silva[45], N. Sagidova[37], B. Saitta[26,f], C. Sanchez Gras[31],

C. Sanchez Mayordomo[46], B. Sanmartin Sedes[45], R. Santacesaria[30], C. Santamarina Rios[45],

M. Santimaria[22], E. Santovetti[29,j], G. Sarpis[61], A. Sarti[30], C. Satriano[30,s], A. Satta[29], M. Saur[5],

D. Savrina[38,39], L. G. Scantlebury Smead[62], S. Schael[13], M. Schellenberg[14], M. Schiller[58],

H. Schindler[47], M. Schmelling[15], T. Schmelzer[14], B. Schmidt[47], O. Schneider[48], A. Schopper[47],

H. F. Schreiner[64], M. Schubiger[31], S. Schulte[48], M. H. Schune[11], R. Schwemmer[47], B. Sciascia[22],

A. Sciubba[30,k], S. Sellam[68], A. Semennikov[38], A. Sergi[52,47], N. Serra[49], J. Serrano[10], L. Sestini[27],

A. Seuthe[14], P. Seyfert[47], D. M. Shangase[79], M. Shapkin[43], T. Shears[59], L. Shekhtman[42,x],

V. Shevchenko[75,76], E. Shmanin[76], J. D. Shupperd[67], B. G. Siddi[20], R. Silva Coutinho[49],

L. Silva de Oliveira[2], G. Simi[27,o], S. Simone[18,d], I. Skiba[20], N. Skidmore[16], T. Skwarnicki[67],

M. W. Slater[52], J. G. Smeaton[54], A. Smetkina[38], E. Smith[13], I. T. Smith[57], M. Smith[60], A. Snoch[31],

M. Soares[19], L. Soares Lavra[1], M. D. Sokoloff[64], F. J. P. Soler[58], B. Souza De Paula[2], B. Spaan[14],

E. Spadaro Norella[25,q], P. Spradlin[58], F. Stagni[47], M. Stahl[64], S. Stahl[47], P. Stefko[48], S. Stefkova[60],

O. Steinkamp[49], S. Stemmle[16], O. Stenyakin[43], M. Stepanova[37], H. Stevens[14], A. Stocchi[11], S. Stone[67],

S. Stracka[28], M. E. Stramaglia[48], M. Straticiuc[36], U. Straumann[49], S. Strokov[78], J. Sun[3], L. Sun[71],

Y. Sun[65], P. Svihra[61], K. Swientek[34], A. Szabelski[35], T. Szumlak[34], M. Szymanski[5], S. Taneja[61],

Z. Tang[3], T. Tekampe[14], G. Tellarini[20], F. Teubert[47], E. Thomas[47], K. A. Thomson[59], M. J. Tilley[60],

V. Tisserand[9], S. T'Jampens[8], M. Tobin[6], S. Tolk[47], L. Tomassetti[20,g], D. Tonelli[28], D. Y. Tou[12],

E. Tournefier[8], M. Traill[58], M. T. Tran[48], A. Trisovic[54], A. Tsaregorodtsev[10], G. Tuci[28,47,p], A. Tully[48],

N. Tuning[31], A. Ukleja[35], A. Usachov[11], A. Ustyuzhanin[41,77], U. Uwer[16], A. Vagner[78], V. Vagnoni[19],

A. Valassi[47], G. Valenti[19], M. van Beuzekom[31], H. Van Hecke[66], E. van Herwijnen[47], C. B. Van Hulse[17],

J. van Tilburg[31], M. van Veghel[74], R. Vazquez Gomez[47], P. Vazquez Regueiro[45], C. Vázquez Sierra[31],

S. Vecchi[20], J. J. Velthuis[53], M. Veltri[21,r], A. Venkateswaran[67], M. Vernet[9], M. Veronesi[31],

M. Vesterinen[55], J. V. Viana Barbosa[47], D. Vieira[5], M. Vieites Diaz[48], H. Viemann[73],

X. Vilasis-Cardona[44,m], A. Vitkovskiy[31], V. Volkov[39], A. Vollhardt[49], D. Vom Bruch[12], A. Vorobyev[37],

V. Vorobyev[42,x], N. Voropaev[37], R. Waldi[73], J. Walsh[28], J. Wang[3], J. Wang[6], M. Wang[3], Y. Wang[7],

Z. Wang[49], D. R. Ward[54], H. M. Wark[59], N. K. Watson[52], D. Websdale[60], A. Weiden[49], C. Weisser[63],

B. D. C. Westhenry[53], D. J. White[61], M. Whitehead[13], D. Wiedner[14], G. Wilkinson[62], M. Wilkinson[67],

I. Williams[54], M. Williams[63], M. R. J. Williams[61], T. Williams[52], F. F. Wilson[56], M. Winn[11],

W. Wislicki[35], M. Witek[33], G. Wormser[11], S. A. Wotton[54], H. Wu[67], K. Wyllie[47], Z. Xiang[5], D. Xiao[7],

Y. Xie[7], H. Xing[70], A. Xu[3], L. Xu[3], M. Xu[7], Q. Xu[5], Z. Xu[8], Z. Xu[3], Z. Yang[3], Z. Yang[65], Y. Yao[67],

L. E. Yeomans[59], H. Yin[7], J. Yu[7,aa], X. Yuan[67], O. Yushchenko[43], K. A. Zarebski[52], M. Zavertyaev[15,c],

M. Zdybal[33], M. Zeng[3], D. Zhang[7], L. Zhang[3], S. Zhang[3], W. C. Zhang[3,z], Y. Zhang[47], A. Zhelezov[16],

Y. Zheng[5], X. Zhou[5], Y. Zhou[5], X. Zhu[3], V. Zhukov[13,39], J. B. Zonneveld[57], and S. Zucchelli[19,e]

[1] *Centro Brasileiro de Pesquisas Físicas (CBPF), Rio de Janeiro, Brazil;*
[2] *Universidade Federal do Rio de Janeiro (UFRJ), Rio de Janeiro, Brazil;*
[3] *Center for High Energy Physics, Tsinghua University, Beijing, China;*
[4] *School of Physics State Key Laboratory of Nuclear Physics and Technology, Peking University, Beijing, China;*
[5] *University of Chinese Academy of Sciences, Beijing, China;*
[6] *Institute Of High Energy Physics (IHEP), Beijing, China;*
[7] *Institute of Particle Physics, Central China Normal University, Wuhan, Hubei, China;*
[8] *Univ. Grenoble Alpes, Univ. Savoie Mont Blanc, CNRS, IN2P3-LAPP, Annecy, France;*
[9] *Université Clermont Auvergne, CNRS/IN2P3, LPC, Clermont-Ferrand, France;*
[10] *Aix Marseille Univ, CNRS/IN2P3, CPPM, Marseille, France;*
[11] *LAL, Univ. Paris-Sud, CNRS/IN2P3, Université Paris-Saclay, Orsay, France;*
[12] *LPNHE, Sorbonne Université Paris Diderot Sorbonne Paris Cité CNRS/IN2P3, Paris, France;*
[13] *I. Physikalisches Institut, RWTH Aachen University, Aachen, Germany;*
[14] *Fakultät Physik, Technische Universität Dortmund, Dortmund, Germany;*
[15] *Max-Planck-Institut für Kernphysik (MPIK), Heidelberg, Germany;*
[16] *Physikalisches Institut, Ruprecht-Karls-Universität Heidelberg, Heidelberg, Germany;*
[17] *School of Physics, University College Dublin, Dublin, Ireland;*
[18] *INFN Sezione di Bari, Bari, Italy;*
[19] *INFN Sezione di Bologna, Bologna, Italy;*
[20] *INFN Sezione di Ferrara, Ferrara, Italy;*
[21] *INFN Sezione di Firenze, Firenze, Italy;*
[22] *INFN Laboratori Nazionali di Frascati, Frascati, Italy;*
[23] *INFN Sezione di Genova, Genova, Italy;*
[24] *INFN Sezione di Milano-Bicocca, Milano, Italy;*
[25] *INFN Sezione di Milano, Milano, Italy;*
[26] *INFN Sezione di Cagliari, Monserrato, Italy;*
[27] *INFN Sezione di Padova, Padova, Italy;*
[28] *INFN Sezione di Pisa, Pisa, Italy;*
[29] *INFN Sezione di Roma Tor Vergata, Roma, Italy;*
[30] *INFN Sezione di Roma La Sapienza, Roma, Italy;*
[31] *Nikhef National Institute for Subatomic Physics, Amsterdam, Netherlands;*
[32] *Nikhef National Institute for Subatomic Physics and VU University Amsterdam, Amsterdam, Netherlands;*
[33] *Henryk Niewodniczanski Institute of Nuclear Physics Polish Academy of Sciences, Kraków, Poland;*
[34] *AGH-University of Science and Technology, Faculty of Physics and Applied Computer Science, Kraków, Poland;*
[35] *National Center for Nuclear Research (NCBJ), Warsaw, Poland;*
[36] *Horia Hulubei National Institute of Physics and Nuclear Engineering, Bucharest-Magurele, Romania;*
[37] *Petersburg Nuclear Physics Institute NRC Kurchatov Institute (PNPI NRC KI), Gatchina, Russia;*
[38] *Institute of Theoretical and Experimental Physics NRC Kurchatov Institute (ITEP NRC KI), Moscow, Russia, Moscow, Russia;*
[39] *Institute of Nuclear Physics, Moscow State University (SINP MSU), Moscow, Russia;*
[40] *Institute for Nuclear Research of the Russian Academy of Sciences (INR RAS), Moscow, Russia;*
[41] *Yandex School of Data Analysis, Moscow, Russia;*
[42] *Budker Institute of Nuclear Physics (SB RAS), Novosibirsk, Russia;*
[43] *Institute for High Energy Physics NRC Kurchatov Institute (IHEP NRC KI), Protvino, Russia, Protvino, Russia;*
[44] *ICCUB, Universitat de Barcelona, Barcelona, Spain;*
[45] *Instituto Galego de Física de Altas Enerxías (IGFAE), Universidade de Santiago de Compostela, Santiago de Compostela, Spain;*
[46] *Instituto de Fisica Corpuscular, Centro Mixto Universidad de Valencia-CSIC, Valencia, Spain;*
[47] *European Organization for Nuclear Research (CERN), Geneva, Switzerland;*
[48] *Institute of Physics, Ecole Polytechnique Fédérale de Lausanne (EPFL), Lausanne, Switzerland;*
[49] *Physik-Institut, Universität Zürich, Zürich, Switzerland;*
[50] *NSC Kharkiv Institute of Physics and Technology (NSC KIPT), Kharkiv, Ukraine;*
[51] *Institute for Nuclear Research of the National Academy of Sciences (KINR), Kyiv, Ukraine;*
[52] *University of Birmingham, Birmingham, United Kingdom;*
[53] *H.H. Wills Physics Laboratory, University of Bristol, Bristol, United Kingdom;*
[54] *Cavendish Laboratory, University of Cambridge, Cambridge, United Kingdom;*
[55] *Department of Physics, University of Warwick, Coventry, United Kingdom;*
[56] *STFC Rutherford Appleton Laboratory, Didcot, United Kingdom;*
[57] *School of Physics and Astronomy, University of Edinburgh, Edinburgh, United Kingdom;*
[58] *School of Physics and Astronomy, University of Glasgow, Glasgow, United Kingdom;*
[59] *Oliver Lodge Laboratory, University of Liverpool, Liverpool, United Kingdom;*
[60] *Imperial College London, London, United Kingdom;*
[61] *Department of Physics and Astronomy, University of Manchester, Manchester, United Kingdom;*
[62] *Department of Physics, University of Oxford, Oxford, United Kingdom;*

[63] *Massachusetts Institute of Technology, Cambridge, MA, United States;*
[64] *University of Cincinnati, Cincinnati, OH, United States;*
[65] *University of Maryland, College Park, MD, United States;*
[66] *Los Alamos National Laboratory (LANL), Los Alamos, United States;*
[67] *Syracuse University, Syracuse, NY, United States;*
[68] *Laboratory of Mathematical and Subatomic Physics , Constantine, Algeria, associated to [2];*
[69] *Pontifícia Universidade Católica do Rio de Janeiro (PUC-Rio), Rio de Janeiro, Brazil, associated to [2];*
[70] *South China Normal University, Guangzhou, China, associated to [3];*
[71] *School of Physics and Technology, Wuhan University, Wuhan, China, associated to [3];*
[72] *Departamento de Fisica, Universidad Nacional de Colombia, Bogota, Colombia, associated to [12];*
[73] *Institut für Physik, Universität Rostock, Rostock, Germany, associated to [16];*
[74] *Van Swinderen Institute, University of Groningen, Groningen, Netherlands, associated to [31];*
[75] *National Research Centre Kurchatov Institute, Moscow, Russia, associated to [38];*
[76] *National University of Science and Technology "MISIS", Moscow, Russia, associated to [38];*
[77] *National Research University Higher School of Economics, Moscow, Russia, associated to [41];*
[78] *National Research Tomsk Polytechnic University, Tomsk, Russia, associated to [38];*
[79] *University of Michigan, Ann Arbor, United States, associated to [67];*

[a] *Universidade Federal do Triângulo Mineiro (UFTM), Uberaba-MG, Brazil;*
[b] *Laboratoire Leprince-Ringuet, Palaiseau, France;*
[c] *P.N. Lebedev Physical Institute, Russian Academy of Science (LPI RAS), Moscow, Russia;*
[d] *Università di Bari, Bari, Italy;*
[e] *Università di Bologna, Bologna, Italy;*
[f] *Università di Cagliari, Cagliari, Italy;*
[g] *Università di Ferrara, Ferrara, Italy;*
[h] *Università di Genova, Genova, Italy;*
[i] *Università di Milano Bicocca, Milano, Italy;*
[j] *Università di Roma Tor Vergata, Roma, Italy;*
[k] *Università di Roma La Sapienza, Roma, Italy;*
[l] *AGH - University of Science and Technology, Faculty of Computer Science, Electronics and Telecommunications, Kraków, Poland;*
[m] *LIFAELS, La Salle, Universitat Ramon Llull, Barcelona, Spain;*
[n] *Hanoi University of Science, Hanoi, Vietnam;*
[o] *Università di Padova, Padova, Italy;*
[p] *Università di Pisa, Pisa, Italy;*
[q] *Università degli Studi di Milano, Milano, Italy;*
[r] *Università di Urbino, Urbino, Italy;*
[s] *Università della Basilicata, Potenza, Italy;*
[t] *Scuola Normale Superiore, Pisa, Italy;*
[u] *Università di Modena e Reggio Emilia, Modena, Italy;*
[v] *Università di Siena, Siena, Italy;*
[w] *MSU-Iligan Institute of Technology (MSU-IIT), Iligan, Philippines;*
[x] *Novosibirsk State University, Novosibirsk, Russia;*
[y] *Sezione INFN di Trieste, Trieste, Italy;*
[z] *School of Physics and Information Technology, Shaanxi Normal University (SNNU), Xi'an, China;*
[aa] *Physics and Micro Electronic College, Hunan University, Changsha City, China;*
[ab] *Lanzhou University, Lanzhou, China;*

[†]*Deceased*

A search for the doubly charmed baryon Ξ_{cc}^+ is performed through its decay to the $\Lambda_c^+ K^- \pi^+$ final state, using proton-proton collision data collected with the LHCb detector at centre-of-mass energies of 7, 8 and 13 TeV. The data correspond to a total integrated luminosity of 9 fb^{-1}. No significant signal is observed in the mass range from 3.4 to 3.8 GeV/c^2. Upper limits are set at 95% credibility level on the ratio of the Ξ_{cc}^+ production cross-section times the branching fraction to that of Λ_c^+ and Ξ_{cc}^{++} baryons. The limits are determined as functions of the Ξ_{cc}^+ mass for different lifetime hypotheses, in the rapidity range from 2.0 to 4.5 and the transverse momentum range from 4 to 15 GeV/c.

charmed baryons, limits on production of particles, charmed quarks, experimental tests

PACS number(s): 14.20.Lq, 13.85.Rm, 14.65.Dw, 12.38.Qk

1 Introduction

The constituent quark model [1-3] predicts the existence of weakly decaying doubly charmed baryons with spin-parity $J^P = 1/2^+$. These include one isospin doublet Ξ_{cc} ($\Xi_{cc}^+ = ccd$ and $\Xi_{cc}^{++} = ccu$), and one isospin singlet Ω_{cc} ($\Omega_{cc}^+ = ccs$). The masses of the two Ξ_{cc} states are predicted to be in the range from 3500 to 3700 MeV/c^2 [4-31], with an isospin splitting of a few MeV/c^2 [32-34]. Predictions of the Ξ_{cc}^+ lifetime span the range of 50 to 250 fs, while the Ξ_{cc}^{++} lifetime is predicted to be three to four times larger due to the W-exchange contribution in the Ξ_{cc}^+ decay and the destructive Pauli interference in the Ξ_{cc}^{++} decay [5, 11, 12, 23, 35-40].

Doubly charmed baryons have been searched for by several experiments in the past decades. The SELEX collaboration reported the observation of the Ξ_{cc}^+ baryon decaying into $\Lambda_c^+ K^- \pi^+$ and $p D^+ K^-$ final states [41, 42], using a 600 GeV/c charged hyperon beam impinging on a fixed target. The mass of the Ξ_{cc}^+ baryon, averaged over the two decay modes, was found to be (3518.7 ± 1.7) MeV/c^2. The lifetime was measured to be less than 33 fs at 90% confidence level. It was estimated that about 20% of Λ_c^+ baryons in the SELEX experiment were produced from Ξ_{cc}^+ decays [41]. Searches in different production environments by the FOCUS [43], BABAR [44], LHCb [45] and Belle [46] experiments did not confirm the SELEX results. Recently, the Ξ_{cc}^{++} baryon was observed by the LHCb experiment in the $\Lambda_c^+ K^- \pi^+ \pi^+$ final state [47], and confirmed in the $\Xi_c^+ \pi^+$ final state [48]. The weighted average of the Ξ_{cc}^{++} mass of the two decay modes was determined to be $(3621.24 \pm 0.65\,(\text{stat}) \pm 0.31\,(\text{syst}))$ MeV/c^2 [48], which is about 100 MeV/c^2 higher than the mass of the Ξ_{cc}^+ baryon reported by SELEX. The lifetime of the Ξ_{cc}^{++} baryon was measured to be $(0.256\,^{+0.024}_{-0.022}\,(\text{stat}) \pm 0.014\,(\text{syst}))$ ps [49], which established its weakly decaying nature. The $\Xi_{cc}^{++} \to D^+ p K^- \pi^+$ decay has been searched for by the LHCb collaboration with a data sample corresponding to an integrated luminosity of 1.7 fb^{-1}, but no signal was found [50].

This paper presents the result of a search for the Ξ_{cc}^+ baryon in the mass range from 3400 to 3800 MeV/c^2, where the Ξ_{cc}^+ baryon is reconstructed through the $\Xi_{cc}^+ \to \Lambda_c^+ K^- \pi^+$, $\Lambda_c^+ \to p K^- \pi^+$ decay chain. The inclusion of charge-conjugate decay processes is implied throughout this paper. The data set comprises pp collision data recorded with the LHCb detector at centre-of-mass energies $\sqrt{s} = 7$ TeV in 2011, $\sqrt{s} = 8$ TeV in 2012 and $\sqrt{s} = 13$ TeV in 2015-2018, corresponding to an integrated luminosity of 1.1 fb^{-1}, 2.1 fb^{-1} and 5.9 fb^{-1}, respectively. This data sample is about ten times larger than that of the previous Ξ_{cc}^+ search by the LHCb collaboration using only 2011 data [45].

The search was performed with the whole analysis procedure defined before inspecting the data in the 3400 to 3800 MeV/c^2 mass range. The analysis strategy is defined as follows: first a search for a Ξ_{cc}^+ signal is performed and the significance of the signal as a function of the Ξ_{cc}^+ mass is evaluated; then if the global significance, after considering the look-elsewhere effect, is above 3 standard deviations, the Ξ_{cc}^+ mass is measured; otherwise, upper limits are set on the production rates for different centre-of-mass energies. Two sets of selections, with different multivariate classifiers and trigger requirements, denoted as Selection A and Selection B are used in these two cases. Selection A is used in the signal search and is designed to maximise its sensitivity. Selection B is optimised for setting upper limits on the ratio of the Ξ_{cc}^+ production rate to that of Ξ_{cc}^{++} and Λ_c^+ baryons. It uses the same selection for Λ_c^+ baryons from Ξ_{cc} decays and prompt Λ_c^+ baryons in order to have better control over sources of systematic uncertainty on the ratio. For the limit setting, only the data recorded at $\sqrt{s} = 8$ TeV in 2012 and at $\sqrt{s} = 13$ TeV in 2016-2018 is used. The 2015 data is excluded because there were significant variations in trigger thresholds during this data-taking period, and because this sample only accounts for 6% of the pp collision data at $\sqrt{s} = 13$ TeV. The production ratio, $\mathcal{R}$, is defined as:

$$\mathcal{R}(\Lambda_c^+) \equiv \frac{\sigma(\Xi_{cc}^+) \times \mathcal{B}(\Xi_{cc}^+ \to \Lambda_c^+ K^- \pi^+)}{\sigma(\Lambda_c^+)} \tag{1}$$

relative to the prompt Λ_c^+ baryons decaying to $p K^- \pi^+$, and

$$\mathcal{R}(\Xi_{cc}^{++}) \equiv \frac{\sigma(\Xi_{cc}^+) \times \mathcal{B}(\Xi_{cc}^+ \to \Lambda_c^+ K^- \pi^+)}{\sigma(\Xi_{cc}^{++}) \times \mathcal{B}(\Xi_{cc}^{++} \to \Lambda_c^+ K^- \pi^+ \pi^+)} \tag{2}$$

relative to the $\Xi_{cc}^{++} \to \Lambda_c^+ K^- \pi^+ \pi^+$ decay, where σ is the production cross-section and $\mathcal{B}$ is the decay branching fraction. The determination of the ratio $\mathcal{R}(\Lambda_c^+)$ allows a direct comparison with previous experiments, while that of $\mathcal{R}(\Xi_{cc}^{++})$ provides information about the ratio of the branching fractions of the $\Xi_{cc}^+ \to \Lambda_c^+ K^- \pi^+$ and $\Xi_{cc}^{++} \to \Lambda_c^+ K^- \pi^+ \pi^+$ decays assuming that the members of the isospin doublet have a similar production cross-section [12, 51, 52]. The production ratios are evaluated as:

$$\mathcal{R} = \frac{\varepsilon_{\text{norm}}}{\varepsilon_{\text{sig}}} \frac{N_{\text{sig}}}{N_{\text{norm}}} \equiv \alpha N_{\text{sig}}, \tag{3}$$

where ε_{sig} and $\varepsilon_{\text{norm}}$ refer to the selection efficiencies of the Ξ_{cc}^+ signal decay mode and the Λ_c^+ or Ξ_{cc}^{++} normalisation decay modes respectively, N_{sig} and N_{norm} are the corresponding yields, and α is the single-event sensitivity. Because the Ξ_{cc}^+ selection efficiency depends strongly on the lifetime, limits on $\mathcal{R}(\Lambda_c^+)$ and $\mathcal{R}(\Xi_{cc}^{++})$ are quoted as functions of the Ξ_{cc}^+ signal mass for a discrete set of lifetime hypotheses.

2 Detector and simulation

The LHCb detector [53, 54] is a single-arm forward spectrometer covering the pseudorapidity range $2 < \eta < 5$, designed for the study of particles containing b or c quarks. The detector includes a high-precision tracking system consisting of a silicon-strip vertex detector surrounding the pp interaction region [55], a large-area silicon-strip detector located upstream of a dipole magnet with a bending power of about 4 Tm, and three stations of silicon-strip detectors and straw drift tubes [56, 57] placed downstream of the magnet. The tracking system provides a measurement of the momentum, p, of charged particles with a relative uncertainty that varies from 0.5% at low momentum to 1.0% at 200 GeV/c. The minimum distance of a track to a primary vertex (PV), the impact parameter (IP), is measured with a resolution of $(15 + 29/p_T)\,\mu\text{m}$, where p_T is the component of the momentum transverse to the beam, in GeV/c. Different types of charged hadrons are distinguished using information from two ring-imaging Cherenkov detectors [58]. The online event selection is performed by a trigger [59], which consists of a hardware stage, based on information from the calorimeter and muon systems, followed by a software stage, which applies a full event reconstruction.

Simulated samples are required to develop the event selection and to estimate the efficiency of the detector acceptance and the imposed selection requirements. Simulated pp collisions are generated using PYTHIA [60, 61] with a specific LHCb configuration [62]. A dedicated generator, GENXICC2.0 [63], is used to simulate the Ξ_{cc} baryon production. Decays of unstable particles are described by EVTGEN [64] in which final-state radiation is generated using PHOTOS [65]. The interaction of the generated particles with the detector, and its response, are implemented using the GEANT4 toolkit [66, 67] as described in ref. [68]. Unless otherwise stated, simulated events are generated with a Ξ_{cc} mass of 3621 MeV/c^2 and a Ξ_{cc}^+ (Ξ_{cc}^{++}) lifetime of 80 fs (256 fs).

3 Reconstruction and selection

For the Ξ_{cc}^+ signal and each of the normalisation modes, Λ_c^+ candidates are reconstructed in the $pK^-\pi^+$ final state. At least one of the three Λ_c^+ decay products is required to pass an inclusive software trigger, which requires that a track with associated large transverse momentum is inconsistent with originating from any PV. For data recorded at $\sqrt{s} = 13$ TeV, at least one of the three Λ_c^+ decay products is required to pass a multivariate selection applied at the software trigger level [69, 70]. The χ_{IP}^2 is defined as the difference in χ^2 of the PV fit with and without the particle in question. The PV of any single particle is defined to be that with respect to which the particle has the smallest χ_{IP}^2. Candidate Λ_c^+ baryons are formed from the combination of three tracks of good quality that do not originate from any PV and have large transverse momentum. Particle identification (PID) requirements are imposed on all three tracks to suppress combinatorial background and misidentified charm-meson decays. The Λ_c^+ candidates are also required to have a mass in the range from 2211 to 2362 MeV/c^2.

The Ξ_{cc}^+ candidates are reconstructed by combining a Λ_c^+ candidate with two tracks, identified as K^- and π^+ mesons using PID information. The kaon and pion tracks are required to have a large transverse momentum and a good track quality. To suppress duplicate tracks, the angle between each pair of the five final-state tracks with the same charge is required to be larger than 0.5 mrad. The Ξ_{cc}^+ candidate is required to have $p_T > 4$ GeV/c and to originate from a PV. Similar requirements are imposed to reconstruct the Ξ_{cc}^{++} candidates in the Ξ_{cc}^{++} normalisation mode, with an additional charged pion in the final state.

Multivariate classifiers based on the gradient boosted decision tree (BDTG) [71-73] are developed to further improve the signal purity. To train the classifier, simulated Ξ_{cc}^+ events are used as the signal sample and wrong-sign (WS) $\Lambda_c^+K^-\pi^-$ combinations selected from the data sample are used as the background sample. For Selection A, the classifier is trained using candidates with a Λ_c^+ mass in the window of 2270 to 2306 MeV/c^2 (corresponding to ± 3 times the resolution on the Λ_c^+ mass) and a Ξ_{cc}^+ mass in the signal search region. Eighteen input variables that show good discrimination for Ξ_{cc}^+ and intermediate Λ_c^+ candidates between signal and background samples are used in the training. These variables can be subdivided into two sets; in the choice of the first set of variables, no strong assumptions are made about the source of the Λ_c^+ candidates, while for the second set of variables the properties of the Ξ_{cc}^+ candidates as the source of the Λ_c^+ candidates are exploited. The first set of variables are: the χ^2 per degree of freedom of the Λ_c^+ vertex fit; the p_T of the Λ_c^+ candidate and of its decay products; and the flight-distance χ^2 between the PV and the decay vertex of the Λ_c^+ candidate. The second set of variables are: the χ^2 per degree of freedom of the Ξ_{cc}^+ vertex fit and of the kinematic refit [74] of the decay chain requiring Ξ_{cc}^+ to originate from its PV; the largest distance of closest approach (DOCA) between the decay products of the Ξ_{cc}^+ candidate; the p_T of the Ξ_{cc}^+ candidate, and of the kaon and pion from the Ξ_{cc}^+ decay; the χ_{IP}^2 of the Ξ_{cc}^+ and Λ_c^+ candidates, and of the K^- and π^+ mesons from the Ξ_{cc}^+ decay; the angle between the momentum and displacement vector of the Ξ_{cc}^+ candidate; and the flight-distance χ^2 between the PV and the decay vertex of the Ξ_{cc}^+ candidate. For Selection B, the multivariate selection comprises two stages. In the first

stage, one classifier is trained with Λ_c^+ signal in the simulated Ξ_{cc}^+ sample and background candidates in the Λ_c^+ mass sideband, and is applied to both the signal mode and the Λ_c^+ normalisation mode. The same input variables are used as for the first set of variables in Selection A, with four additional variables that enhance the discriminating power: the largest DOCA between the decay products of the Λ_c^+ candidate and the χ_{IP}^2 of the decay products of the Λ_c^+ candidate. In the second stage, another classifier is trained for the signal mode using candidates in the mass window of the intermediate Λ_c^+ and the Ξ_{cc}^+ signal search region. Candidates used in the training are also required to pass a BDTG response threshold of the first classifier. The input variables are those from the second set of Selection A with an additional variable, the angle between the momentum and displacement vector of the Λ_c^+ candidate.

The thresholds of the BDTG responses for both Selections A and B are determined by maximising the expected value of the figure of merit $\varepsilon/\left(\frac{5}{2} + \sqrt{N_{\mathrm{B}}}\right)$ [75], where ε is the estimated signal efficiency, 5/2 corresponds to 5 standard deviations in a Gaussian significance test, and N_{B} the expected number of background candidates under the signal peak. The quantity N_{B} is estimated with the WS control sample in the mass region of $\pm 12.5\,\mathrm{MeV}/c^2$ around the known Ξ_{cc}^{++} mass [76], taking into account the difference of the background level for the signal sample and the WS control sample. The performance of the BDTG classifier is tested and found to be stable against the Ξ_{cc}^+ lifetimes in the range from 40 to 120 fs. Following the same procedure, a two-stage multivariate selection is developed for the Ξ_{cc}^{++} normalisation mode.

Events that pass the multivariate selection may contain more than one Ξ_{cc}^+ candidate in the search region although the probability to produce more than one Ξ_{cc}^+ is small. According to studies of simulated decays and the WS control sample, multiple candidates in the same event do not form a peaking background except for one case in which the candidates are obtained from the same five final-state tracks, but with two tracks interchanged (e.g. the K^- from the Λ_c^+ decay and the K^- from the Ξ_{cc}^+ decay). In this case, only one candidate is chosen randomly.

For Selection B, an additional hardware trigger requirement is imposed on candidates of both the signal and the normalisation mode to minimise systematic differences in efficiency between the modes. This hardware trigger requirement selects candidates in which at least one of the three Λ_c^+ decay products deposits high transverse energy in the calorimeters. Finally, Ξ_{cc}^+ baryon candidates in the signal mode and Λ_c^+ and Ξ_{cc}^{++} baryons in the normalisation modes are required to be reconstructed in the fiducial region of rapidity $2.0 < y < 4.5$ and transverse momentum $4 < p_{\mathrm{T}} < 15\,\mathrm{GeV}/c$.

4 Yield measurements

Selection A described above is applied to the full data sample. Figure 1 shows the $M([pK^-\pi^+]_{\Lambda_c^+})$ and $m(\Lambda_c^+ K^-\pi^+)$ distributions in the Λ_c^+ mass range from 2270 to 2306 MeV/c^2. The quantity $m(\Lambda_c^+ K^-\pi^+)$ is defined as:

$$m(\Lambda_c^+ K^-\pi^+) \equiv M([pK^-\pi^+]_{\Lambda_c^+} K^-\pi^+) - M([pK^-\pi^+]_{\Lambda_c^+})$$
$$+ M_{\mathrm{PDG}}(\Lambda_c^+), \qquad (4)$$

where $M([pK^-\pi^+]_{\Lambda_c^+} K^-\pi^+)$ is the reconstructed mass of the Ξ_{cc}^+ candidate, $M([pK^-\pi^+]_{\Lambda_c^+})$ is the reconstructed mass of the Λ_c^+ candidate, and $M_{\mathrm{PDG}}(\Lambda_c^+)$ is the known value of the Λ_c^+ mass [76]. As a comparison, the $m(\Lambda_c^+ K^-\pi^-)$ distribution of the WS control sample is also shown in Figure 1(b). The dotted red line indicates the mass of the Ξ_{cc}^+ baryon reported by SELEX [41, 42], and the dashed blue line refers to the mass of the Ξ_{cc}^{++} baryon [47, 48]. The small enhancement below 3500 MeV/c^2, compared to the WS sample, is due to partially reconstructed Ξ_{cc}^{++} decays. There is no excess near a mass of 3520 MeV/c^2. A small enhancement is seen near a mass of 3620 MeV/c^2. To determine the statistical significance of this
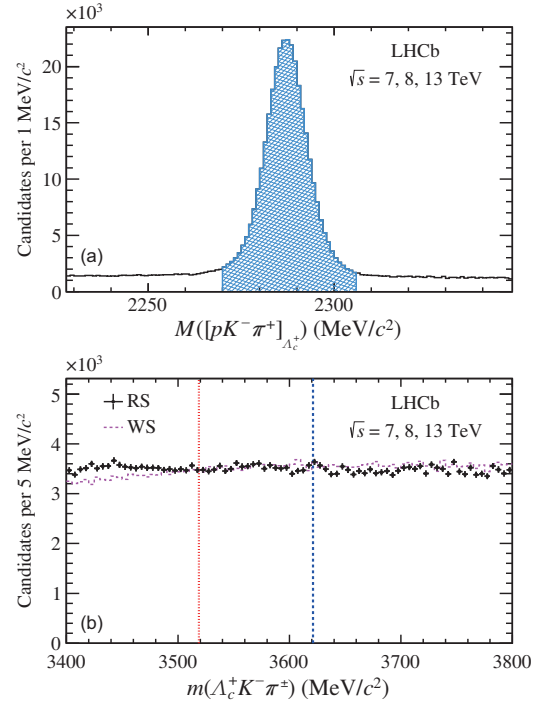

Figure 1 (Color online) Mass distributions of the (a) intermediate Λ_c^+ and (b) Ξ_{cc}^+ candidates for the full data sample. Selection A is applied, including the Λ_c^+ mass requirement, indicated by the cross-hatched region in plot (a), of 2270 MeV/c^2 < $M([pK^-\pi^+]_{\Lambda_c^+})$ < 2306 MeV/c^2. The right-sign (RS) $m(\Lambda_c^+ K^-\pi^+)$ distribution is shown in plot (b), along with the wrong-sign (WS) $m(\Lambda_c^+ K^-\pi^-)$ distribution normalised to have the same area. The dotted red line at 3518.7 MeV/c^2 indicates the mass of the Ξ_{cc}^+ baryon reported by SELEX [42] and the dashed blue line at 3621.2 MeV/c^2 indicates the mass of the isospin partner, the Ξ_{cc}^{++} baryon [48].

enhancement, an extended unbinned maximum-likelihood fit is performed to the $m(\Lambda_c^+ K^- \pi^+)$ distribution. The signal component is described with the sum of a Gaussian function and a modified Gaussian function with power-law tails on both sides [77]. The parameters of the signal model are fixed from simulation except for the common peak position of the two functions that is allowed to vary freely in the fit. The background component is described by a second-order Chebyshev polynomial with all parameters free. A local p-value is evaluated with the likelihood ratio test for rejection of the background-only hypothesis assuming a positive signal [78,79] and is shown in Figure 2. The largest local significance, corresponding to 3.1 standard deviations (2.7 standard deviations after considering systematic uncertainties), occurs around 3620 MeV/c^2. Taking into account the look-elsewhere effect in the mass range of 3500 to 3700 MeV/c^2 following ref. [80], the global p-value is 4.2×10^{-2}, corresponding to a significance of 1.7 standard deviations. Since no excess above 3 standard deviations is observed, upper limits on the production ratios are set using the data recorded at $\sqrt{s} = 8$ TeV in 2012 and at $\sqrt{s} = 13$ TeV in 2016-2018 after applying Selection B.

To measure the production ratios, it is necessary to determine the yields of the normalisation modes. The yield determination procedure of the prompt Λ_c^+ decays is complicated by the substantial secondary Λ_c^+ contribution from b-hadron decays, and is done in two steps. First, the total number of Λ_c^+ candidates is determined with an extended unbinned maximum-likelihood fit to the $M([pK^-\pi^+]_{\Lambda_c^+})$ distribution. Then, a fit to the $\log_{10}(\chi_{\mathrm{IP}}^2)$ distribution is performed to discriminate between prompt and secondary Λ_c^+ candidates. Information from the Λ_c^+ mass fit is used to constrain the total number of Λ_c^+ candidates. The shapes of the prompt and secondary $\log_{10}(\chi_{\mathrm{IP}}^2)$ distributions are described by a Bukin function [81]. The shape parameters of the prompt and secondary components are determined from simulation, except for the mean and the width parameters of the Bukin function, which are allowed to vary in the fit. The background component is described by a nonparametric function generated using the data from the Λ_c^+ mass sideband regions. As an illustration, the $M([pK^-\pi^+]_{\Lambda_c^+})$ and $\log_{10}(\chi_{\mathrm{IP}}^2)$ distributions of the Λ_c^+ normalisation mode candidates in the 2018 data set are shown in Figure 3. The prompt Λ_c^+ yields are summarised in Table 1.

To determine the Ξ_{cc}^{++} yield, an extended unbinned maximum-likelihood fit is performed to the $m(\Lambda_c^+ K^- \pi^+ \pi^+)$ distribution, which is defined in a similar way to eq. (4). The same signal and background parameterisations are used as for the signal mode. For the data sample recorded at $\sqrt{s} = 13$ TeV, a simultaneous fit is performed to the $m(\Lambda_c^+ K^- \pi^+ \pi^+)$ distributions of the candidates in the 2016, 2017 and 2018 data sets with the shared mean and resolution parameter. As

an illustration, the $m(\Lambda_c^+ K^- \pi^+ \pi^+)$ distribution for the 2018 data set is shown in Figure 4 along with the associated fit result. The Ξ_{cc}^{++} yields are summarised in Table 1.
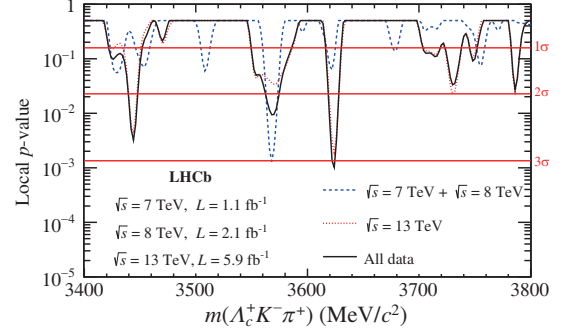

Figure 2 (Color online) Local p-value (statistical only) at different Ξ_{cc}^+ mass values evaluated with the likelihood-ratio test, for the data sets recorded at $\sqrt{s} = 7$ TeV, $\sqrt{s} = 8$ TeV and $\sqrt{s} = 13$ TeV. Selection A is applied, including the Λ_c^+ mass requirement of 2270 MeV/$c^2 < M([pK^-\pi^+]_{\Lambda_c^+}) <$ 2306 MeV/c^2.
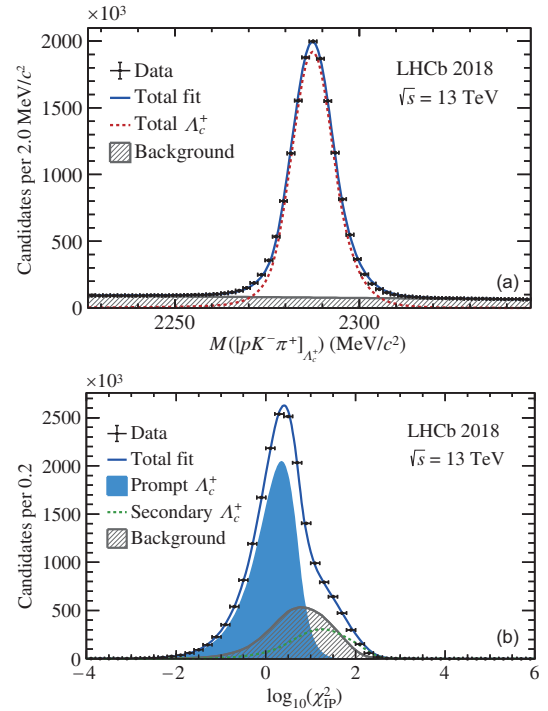

Figure 3 (Color online) Distributions of (a) $M([pK^-\pi^+]_{\Lambda_c^+})$ and (b) $\log_{10}(\chi_{\mathrm{IP}}^2)$ of the selected Λ_c^+ candidates with associated fit results for the 2018 data set.

Table 1 Signal yields for prompt $\Lambda_c^+ \to pK^-\pi^+$ and $\Xi_{cc}^{++} \to \Lambda_c^+ K^-\pi^+\pi^+$ normalisation modes, split by data-taking period. The integrated luminosity $\mathcal{L}$ is also shown for each data-taking period

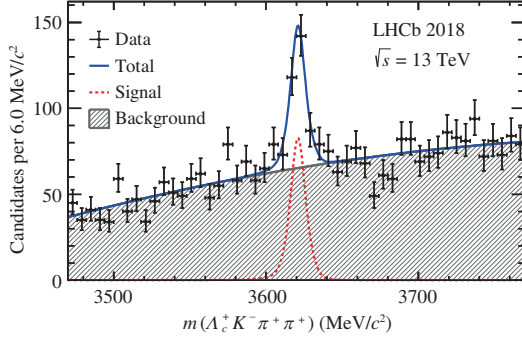| Period	$\mathcal{L}$ (fb^{-1})	$N(\Lambda_c^+)$ ($\times 10^3$)	$N(\Xi_{cc}^{++})$
2012	2.1	1175.3 ± 2.5	38 ± 10
2016	1.7	7339 ± 12	121 ± 19
2017	1.7	9883 ± 9	153 ± 22
2018	2.2	11184 ± 13	188 ± 24

Figure 4   (Color online) Mass distribution of Ξ_{cc}^{++} candidates in the 2018 data set. The result of a fit to the distribution is shown.

5   Efficiency ratio measurement

To set upper limits on the production ratios, the efficiency ratio $\varepsilon_{\text{norm}}/\varepsilon_{\text{sig}}$ is determined from simulation. The signal efficiency is estimated with mass and lifetime hypotheses of $m(\Xi_{cc}^+) = 3621\,\text{MeV}/c^2$ and $\tau(\Xi_{cc}^+) = 80\,\text{fs}$. The kinematic distribution of the Ξ_{cc}^+ baryon is assumed to be the same as for its isospin partner Ξ_{cc}^{++} and the p_{T} distribution of simulated Ξ_{cc}^+ decays is corrected according to the data-simulation discrepancy observed in the Ξ_{cc}^{++} normalisation mode. The Dalitz distributions of the simulated Λ_c^+ decays are corrected to match the distribution observed in background-subtracted data, obtained using the *sPlot* technique [82]. Corrections are applied to the tracking efficiency and PID response of the simulated samples using calibration data samples [83-85]. The efficiency ratio obtained for the Λ_c^+ and Ξ_{cc}^{++} normalisation modes and for different data-taking years are summarised in Table 2, where the uncertainties are due to the limited sizes of the simulated samples. The increase in the efficiency ratio of the Ξ_{cc}^{++} normalisation mode in 2017-2018 compared to that in 2016 is due to the improvement of the online event selection following the observation of the Ξ_{cc}^{++} baryon.

The signal efficiency of the event selection has a strong dependence on the Ξ_{cc}^+ lifetime. To estimate the efficiency for other lifetime hypotheses, the decay time of the simulated Ξ_{cc}^+ events are weighted to have different exponential distributions and the efficiency is re-calculated. A discrete set of hypotheses (40, 80, 120, and 160 fs) is motivated by the measured Ξ_{cc}^{++} lifetime of 256 fs [49] and the expectation that the Ξ_{cc}^+ lifetime is three to four times smaller than that of the Ξ_{cc}^{++} baryon [5,11,12,23,35-40]. Combining the yields of the normalisation modes obtained in the previous section, the values of the single-event sensitivity of the Λ_c^+ and Ξ_{cc}^{++} modes for several lifetime hypotheses are shown in Tables 3 and 4 respectively. The uncertainties on the single-event sensitivities are due to the limited sizes of the simulated samples and the statistical uncertainties on the measured yields.

Table 2   Efficiency ratios between the normalisation and signal modes for different data-taking periods. The uncertainties are due to the limited size of the simulated samples

Efficiency ratios	2012	2016	2017	2018
$\varepsilon_{\text{norm}}(\Lambda_c^+)/\varepsilon_{\text{sig}}$	54 ± 17	22.0 ± 1.9	22.4 ± 1.3	26.1 ± 1.8
$\varepsilon_{\text{norm}}(\Xi_{cc}^{++})/\varepsilon_{\text{sig}}$	2.1 ± 0.7	1.17 ± 0.11	1.91 ± 0.11	1.99 ± 0.12

Table 3   Single-event sensitivity of the Λ_c^+ normalisation mode $\alpha(\Lambda_c^+)$ ($\times 10^{-5}$) for different lifetime hypotheses of the Ξ_{cc}^+ baryon in the different data-taking years. The uncertainties are due to the limited sizes of the simulated samples and the statistical uncertainties on the measured Λ_c^+ baryon yields

Period	$\tau = 40\,\text{fs}$	$\tau = 80\,\text{fs}$	$\tau = 120\,\text{fs}$	$\tau = 160\,\text{fs}$
2012	14.2 ± 4.8	4.6 ± 1.4	2.65 ± 0.77	1.91 ± 0.53
2016	0.60 ± 0.08	0.29 ± 0.02	0.20 ± 0.01	0.16 ± 0.01
2017	0.46 ± 0.04	0.23 ± 0.01	0.15 ± 0.01	0.12 ± 0.01
2018	0.52 ± 0.04	0.23 ± 0.02	0.15 ± 0.01	0.11 ± 0.01

Table 4   Single-event sensitivity of the Ξ_{cc}^{++} normalisation mode $\alpha(\Xi_{cc}^{++})$ ($\times 10^{-2}$) for different lifetime hypotheses of the Ξ_{cc}^+ baryon in the different data-taking years. The uncertainties are due to the limited size of the simulated samples and the statistical uncertainty on the measured Ξ_{cc}^{++} baryon yield

Period	$\tau = 40\,\text{fs}$	$\tau = 80\,\text{fs}$	$\tau = 120\,\text{fs}$	$\tau = 160\,\text{fs}$
2012	16.7 ± 7.1	5.4 ± 2.2	3.1 ± 1.2	2.3 ± 0.8
2016	1.96 ± 0.42	0.96 ± 0.18	0.65 ± 0.12	0.52 ± 0.09
2017	2.51 ± 0.42	1.25 ± 0.19	0.84 ± 0.13	0.69 ± 0.11
2018	2.36 ± 0.34	1.06 ± 0.15	0.68 ± 0.10	0.52 ± 0.08

The efficiency could depend on the Ξ_{cc}^+ mass, since it affects the kinematic distributions of the decay products of the Ξ_{cc}^+ baryon. To test other mass hypotheses, two simulated samples are generated with $m(\Xi_{cc}^+) = 3518.7\,\text{MeV}/c^2$ and $m(\Xi_{cc}^+) = 3700.0\,\text{MeV}/c^2$. The p_{T} distributions of the three decay products of the Ξ_{cc}^+ in the simulated sample with $m(\Xi_{cc}^+) = 3621.4\,\text{MeV}/c^2$ are weighted to match those in the other mass hypotheses, and the efficiency is re-calculated with the weighted sample. Despite the variations of individual efficiency components, the total efficiency is found to be independent of such variations. The mass dependence can be effectively ignored for the evaluation of the single-event sensitivities.

6   Systematic uncertainties

The systematic uncertainties on the measured production ratio $\mathcal{R}$ are presented in Table 5. The total systematic uncertainty is calculated as the quadratic sum of the individual uncertainties, assuming all sources to be independent.

Table 5   Summary of the systematic uncertainties of the production ratio measurement

Source	$\sqrt{s} = 8$ TeV		$\sqrt{s} = 13$ TeV	
	$\mathcal{R}(\Lambda_c^+)$ (%)	$\mathcal{R}(\Xi_{cc}^{++})$ (%)	$\mathcal{R}(\Lambda_c^+)$ (%)	$\mathcal{R}(\Xi_{cc}^{++})$ (%)
Trigger efficiency	11.7	17.7	4.9	11.2
Yield measurement	5.8	8.9	0.6	0.4
PID efficiency	2.5	4.6	0.9	0.8
Tracking	4.3	2.6	4.4	3.1
Total	14.0	20.5	6.7	11.7

The largest systematic uncertainty arises from the evaluation of the efficiency of the hardware-trigger requirement. The cancellation of the hardware-trigger efficiencies in the ratio of the signal and the normalisation decay channels is studied with the Λ_c^+ and Λ_b^0 control samples, using a tag-and-probe method [59]. The difference between the efficiency ratio in data and in simulation is assigned as systematic uncertainty.

The systematic uncertainty on the yield determination is evaluated by varying the choice of the model used to fit the data. For the $\Xi_{cc}^{++} \to \Lambda_c^+ K^- \pi^+ \pi^+$ decay, an alternative model is used where the signal is described by the sum of two Gaussian functions and the background is described by a second-order polynomial function. For the $\Lambda_c^+ \to p K^- \pi^+$ normalisation mode, the yield of the prompt Λ_c^+ is determined by the fit to the $\log_{10}(\chi_{IP}^2)$ distribution. The uncertainty on the determined signal yield may arise from signal modelling and the limited size of the sample in the background region of the Λ_c^+ invariant mass used to model the background. For the signal modelling, a bifurcated Gaussian with an exponential tail is used. The effect of the background is evaluated through the use of pseudoexperiments. The background population in each bin of the $\log_{10}(\chi_{IP}^2)$ template is fluctuated randomly, and the fit procedure is repeated.

The PID efficiency is determined in bins of particle momentum and pseudorapidity using calibration data samples. The effect of the limited size of the calibration samples is studied with a large number of pseudoexperiments and that of the binning scheme is studied by increasing the number of bins by a factor of two. The sum in quadrature of these effects is taken as systematic uncertainty arising from PID efficiency.

The tracking efficiency is corrected with calibration data samples [83]. There are three sources of systematic uncertainties related to this correction. The first is due to the limited size of the calibration samples and is estimated with pseudoexperiments. The second is due to the calibration method and an uncertainty of 0.8% (0.4%) per track is assigned for the 13 TeV (7 TeV) data [83]. The third is due to the imperfect knowledge of the material budget in the detector. The above contributions to the systematic uncertainty are summed in quadrature.

7   Upper limits

Upper limits at 95% credibility level are set on the production ratio $\mathcal{R}(\Lambda_c^+)$ and $\mathcal{R}(\Xi_{cc}^{++})$ at centre-of-mass energies $\sqrt{s} = 8$ TeV and $\sqrt{s} = 13$ TeV, in the fiducial region of rapidity $2.0 < y < 4.5$ and transverse momentum $4 < p_T < 15$ GeV/c. Upper limits are calculated in 2.5 MeV/c^2 intervals over the $m(\Lambda_c^+ K^- \pi^+)$ mass range of 3400 to 3800 MeV/c^2 for the four different lifetime hypotheses. For each fixed value of the Ξ_{cc}^+ mass and lifetime, the likelihood profile $\mathcal{L}(\mathcal{R})$ is determined as a function of $\mathcal{R}$. The likelihood profile for the data recorded at $\sqrt{s} = 13$ TeV is obtained with a simultaneous fit to the $m(\Lambda_c^+ K^- \pi^+)$ distributions using the same fit model as described in sect. 4. Then the likelihood profile $\mathcal{L}(\mathcal{R})$ is convolved with a Gaussian distribution whose width is equal to the square root of the quadratic combination of the statistical and systematic uncertainty on the single-event sensitivity. The upper limit at 95% credibility level is defined as the value of $\mathcal{R}$ at which the integral starting from zero equals 95% of the total area under the curve. Figures 5 and 6 show the 95% credibility level upper limits at centre-of-mass energies of $\sqrt{s} = 8$ TeV and $\sqrt{s} = 13$ TeV, respectively.

8   Conclusion

A search for the doubly charmed baryon Ξ_{cc}^+ is performed through its decay to $\Lambda_c^+ K^- \pi^+$, with the pp collision data
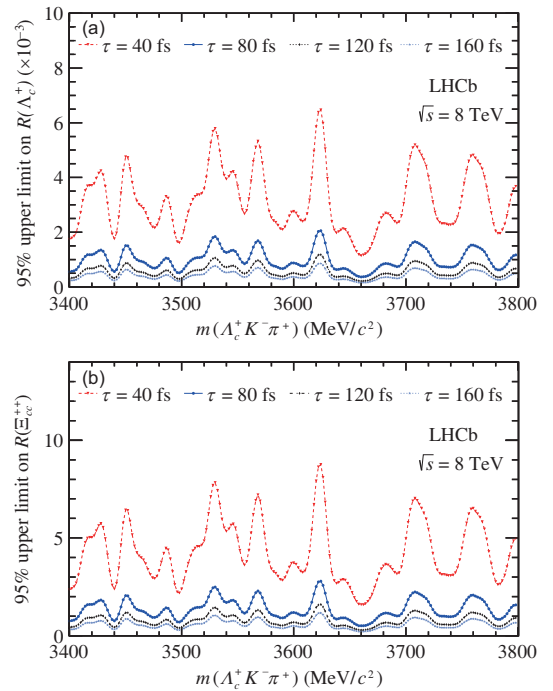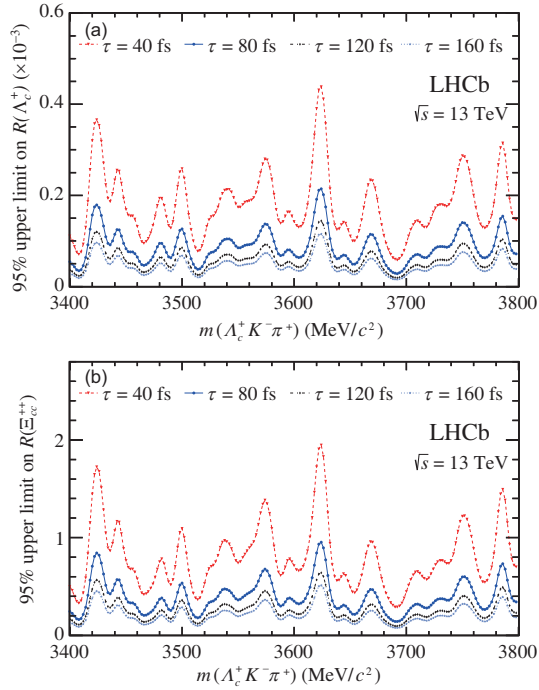

Figure 5   (Color online) Upper limits on (a) $\mathcal{R}(\Lambda_c^+)$ and (b) $\mathcal{R}(\Xi_{cc}^{++})$ at 95% credibility level as a function of $m(\Lambda_c^+ K^- \pi^+)$ at $\sqrt{s} = 8$ TeV for four Ξ_{cc}^+ lifetime hypotheses.

Figure 6 (Color online) Upper limits on (a) $\mathcal{R}(\Lambda_c^+)$ and (b) $\mathcal{R}(\Xi_{cc}^{++})$ at 95% credibility level as a function of $m(\Lambda_c^+ K^- \pi^+)$ at $\sqrt{s} = 13$ TeV, for four Ξ_{cc}^+ lifetime hypotheses.

collected by the LHCb experiment at centre-of-mass energies of 7, 8 and 13 TeV, corresponding to an integrated luminosity of 9 fb^{-1}. No significant signal is observed in the mass range from 3.4 to 3.8 GeV/c^2. Upper limits are set at 95% credibility level on the ratio of the Ξ_{cc}^+ production cross-section times the branching fraction to that of the Λ_c^+ and Ξ_{cc}^{++} baryons. The limits are determined as functions of the Ξ_{cc}^+ mass for different lifetime hypotheses, in the rapidity range from 2.0 to 4.5 and the transverse momentum range from 4 to 15 GeV/c. The upper limit on the production ratio $R(\Lambda_c^+)$ $(R(\Xi_{cc}^{++}))$ depends strongly on the considered mass and lifetime of the Ξ_{cc}^+ baryon, varying from 0.45×10^{-3} (2.0) for 40 fs to 0.12×10^{-3} (0.5) for 160 fs, as summarised in Table 6. The upper limits on $R(\Lambda_c^+)$ are improved by one order of magnitude compared to the previous LHCb search [45] and are significantly below the value reported by SELEX [41], albeit in a different production environment. Future searches by the LHCb

Table 6 Summary of the largest upper limits on production ratios at 95% credibility level for four lifetime hypotheses and different centre-of-mass energies

Lifetime	$\sqrt{s} = 8$ TeV		$\sqrt{s} = 13$ TeV	
(fs)	$\mathcal{R}(\Lambda_c^+)$ ($\times 10^{-3}$)	$\mathcal{R}(\Xi_{cc}^{++})$	$\mathcal{R}(\Lambda_c^+)$ ($\times 10^{-3}$)	$\mathcal{R}(\Xi_{cc}^{++})$
40	6.5	8.8	0.45	2.0
80	2.1	2.8	0.22	1.0
120	1.2	1.6	0.15	0.6
160	0.9	1.2	0.12	0.5

experiment with further improved trigger conditions, additional Ξ_{cc}^+ decay modes, and larger data samples should significantly increase the Ξ_{cc}^+ signal sensitivity.

1 M. Gell-Mann, Phys. Lett. **8** 214 (1964).
2 G. Zweig, *An SU$_3$ Model for Strong Interaction Symmetry and Its Breaking; Version 1*, Technical Report, CERN-TH-401 (CERN, Geneva, 1964).
3 G. Zweig, in *Developments in the Quark Theory of Hadrons, Volume 1*, edited by D. Lichtenberg, and S. Rosen, CERN-TH-412 (CERN, Geneva, 1964), pp. 22-101.
4 B. O. Kerbikov, M. I. Polikarpov, and L. V. Shevchenko, Nucl. Phys. B **331**, 19 (1990).
5 S. Fleck, and J. M. Richard, Prog. Theor. Phys. **82** 760 (1989).
6 S. Chernyshev, M. A. Nowak, and I. Zahed, Phys. Rev. D **53**, 5176 (1996).
7 S. S. Gershtein, V. V. Kiselev, A. K. Likhoded, and A. I. Onishchenko, Mod. Phys. Lett. A **14**, 135 (1999).
8 S. S. Gershtein, V. V. Kiselev, A. K. Likhoded, and A. I. Onishchenko, Phys. Atom. Nuclei **63**, 274 (2000).
9 S. S. Gershtein, V. V. Kiselev, A. K. Likhoded, and A. I. Onishchenko, Phys. Rev. D **62**, 054021 (2000).
10 C. Itoh, T. Minamikawa, K. Miura, and T. Watanabe, Phys. Rev. D **61**, 057502 (2000).
11 K. Anikeev, D. Atwood, F. Azfar, S. Bailey, C. W. Bauer, W. Bell, G. Bodwin, E. Braaten, G. Burdman, J. N. Butler, K. Byrum, N. Cason, A. Cerri, H. W. K. Cheung, A. Dighe, S. Donati, R. K. Ellis, A. Falk, G. Feild, S. Fleming, I. Furic, S. Gardner, Y. Grossman, G. Gutierrez, W. Hao, B. W. Harris, J. Hewett, G. Hiller, R. Jesik, M. Jones, P. A. Kasper, A. El-Khadra, M. Kirk, V. V. Kiselev, J. Kroll, A. S. Kronfeld, R. Kutschke, V. E. Kuznetsov, E. Laenen, J. Lee, A. K. Leibovich, J.

D. Lewis, Z. Ligeti, A. K. Likhoded, H. E. Logan, M. Luke, A. Maciel, G. Majumder, P. Maksimovic, M. Martin, S. Menary, P. Nason, U. Nierste, Y. Nir, L. Nogach, E. Norrbin, C. Oleari, V. Papadimitriou, M. Paulini, C. Paus, M. Petteni, R. Poling, M. Procario, G. Punzi, H. Quinn, A. Rakitine, G. Ridolfi, K. Shestermanov, G. Signorelli, J. P. Silva, T. Skwarnicki, A. Smith, B. Speakman, K. Stenson, F. Stichelbaut, S. Stone, K. Sumorok, M. Tanaka, W. Taylor, W. Trischuk, J. Tseng, R. Van Kooten, A. Vasiliev, M. Voloshin, J. C. Wang, A. B. Wicklund, F. Wurthwein, N. Xuan, J. Yarba, K. Yip, A. Zieminski, in *B physics at the Tevatron: Run II and beyond: Workshop on B Physics at the Tevatron: Run II and Beyond*, Batavia, Illinois, September 23-25 (1999).

12 V. V. Kiselev, and A. K. Likhoded, Phys.-Usp. **45**, 455 (2002).

13 D. Ebert, R. N. Faustov, V. O. Galkin, and A. P. Martynenko, Phys. Rev. D **66**, 014008 (2002).

14 N. Mathur, R. Lewis, and R. M. Woloshyn, Phys. Rev. D **66**, 014502 (2002).

15 D. H. He, K. Qian, Y. B. Ding, X. Q. Li, and P. N. Shen, Phys. Rev. D **70**, 094004 (2004).

16 W. Roberts, and M. Pervin, Int. J. Mod. Phys. A **23**, 2817 (2008), arXiv: 0711.2492.

17 A. Valcarce, H. Garcilazo, and J. Vijande, Eur. Phys. J. A **37**, 217 (2008), arXiv: 0807.2973.

18 J. R. Zhang, and M. Q. Huang, Phys. Rev. D **78**, 094007 (2008), arXiv: 0810.5396.

19 Z. G. Wang, Eur. Phys. J. A **45**, 267 (2010), arXiv: 1001.4693.

20 T. M. Aliev, K. Azizi, and M. Savcı, Nucl. Phys. A **895**, 59 (2012), arXiv: 1205.2873.

21 Y. Namekawa, S. Aoki, K. I. Ishikawa, N. Ishizuka, K. Kanaya, Y. Kuramashi, M. Okawa, Y. Taniguchi, A. Ukawa, N. Ukita, and T. Yoshié, Phys. Rev. D **87**, 094512 (2013), arXiv: 1301.4743.

22 Z. F. Sun, Z. W. Liu, X. Liu, and S. L. Zhu, Phys. Rev. D **91**, 094030 (2015), arXiv: 1411.2117.

23 M. Karliner, and J. L. Rosner, Phys. Rev. D **90**, 094007 (2014), arXiv: 1408.5877.

24 Z. S. Brown, W. Detmold, S. Meinel, and K. Orginos, Phys. Rev. D **90**, 094507 (2014), arXiv: 1409.0497.

25 M. Padmanath, R. G. Edwards, N. Mathur, and M. Peardon, Phys. Rev. D **91**, 094502 (2015), arXiv: 1502.01845.

26 P. Pérez-Rubio, S. Collins, and G. S. Bali, Phys. Rev. D **92**, 034504 (2015), arXiv: 1503.08440.

27 K. W. Wei, B. Chen, and X. H. Guo, Phys. Rev. D **92**, 076008 (2015), arXiv: 1503.05184.

28 Z. F. Sun, and M. J. V. Vacas, Phys. Rev. D **93**, 094002 (2016), arXiv: 1602.04714.

29 C. Alexandrou, and C. Kallidonis, Phys. Rev. D **96**, 034511 (2017), arXiv: 1704.02647.

30 Y. Liu, and I. Zahed, Phys. Rev. D **95**, 116012 (2017), arXiv: 1704.03412.

31 Y. Liu, and I. Zahed, Phys. Rev. D **96**, 056027 (2017), arXiv: 1705.01397.

32 C. W. Hwang, and C. H. Chung, Phys. Rev. D **78**, 073013 (2008), arXiv: 0804.4044.

33 S. J. Brodsky, F. K. Guo, C. Hanhart, and U. G. Meißner, Phys. Lett. B **698**, 251 (2011), arXiv: 1101.1983.

34 M. Karliner, and J. L. Rosner, Phys. Rev. D **96**, 033004 (2017), arXiv: 1706.06961.

35 B. Guberina, B. Melić, and H. Štefančić, Eur. Phys. J. C **9**, 213 (1999).

36 V. V. Kiselev, A. K. Likhoded, and A. I. Onishchenko, Phys. Rev. D **60**, 014007 (1999).

37 A. K. Likhoded, and A. I. Onishchenko, arXiv: hep-ph/9912425.

38 A. I. Onishchenko, in *Inclusive and exclusive decays of doubly heavy baryons: 5th International Workshop on Heavy Quark Physics Dubna*, Russia, April 6-8 (2000).

39 C. H. Chang, T. Li, X. Q. Li, and Y. M. Wang, Commun. Theor. Phys. **49**, 993 (2008), arXiv: 0704.0016.

40 A. V. Berezhnoy, and A. K. Likhoded, Phys. Atom. Nuclei **79**, 260 (2016).

41 M. Mattson, et al. (SELEX Collaboration), Phys. Rev. Lett. **89**, 112001 (2002).

42 A. Ocherashvili, et al. (SELEX Collaboration), Phys. Lett. B **628**, 18 (2005).

43 S. P. Ratti, et al. (FOCUS Collaboration), Nucl. Phys. B-Proc. Suppl. **115**, 33 (2003).

44 B. Aubert, et al. (BABAR Collaboration), Phys. Rev. D **74**, 011103 (2006).

45 R. Aaij, et al. (LHCb Collaboration), J. High Energ. Phys. **2013(12)**, 90 (2013), arXiv: 1310.2538.

46 Y. Kato, et al. (Belle Collaboration), Phys. Rev. D **89**, 052003 (2014), arXiv: 1312.1026.

47 R. Aaij, et al. (LHCb Collaboration), Phys. Rev. Lett. **119**, 112001 (2017).

48 R. Aaij, et al. (LHCb Collaboration), Phys. Rev. Lett. **121**, 162002 (2018).

49 R. Aaij, et al. (LHCb Collaboration), Phys. Rev. Lett. **121**, 052002 (2018).

50 R. Aaij, et al. (LHCb Collaboration), J. High Energ. Phys. **10**, 124 (2019).

51 J. P. Ma, and Z. G. Si, Phys. Lett. B **568**, 135 (2003).

52 C. H. Chang, C. F. Qiao, J. X. Wang, and X. G. Wu, Phys. Rev. D **73**, 094022 (2006).

53 A. A. Alves Jr., et al. (LHCb Collaboration), J. Inst. **3**, S08005 (2008).

54 R. Aaij, et al. (LHCb Collaboration), Int. J. Mod. Phys. A **30**, 1530022 (2015), arXiv: 1412.6352.

55 R. Aaij, et al. (LHCb Collaboration), J. Inst. **9**, P09007 (2014).

56 R. Arink, et al. (LHCb Outer Tracker Group), J. Inst. **9**, P01002 (2014), arXiv: 1311.3893.

57 P. d'Argent, L. Dufour, L. Grillo, J. A. de Vries, A. Ukleja, R. Aaij, F. Archilli, S. Bachmann, D. Berninghoff, A. Birnkraut, J. Blouw, M. D. Cian, G. Ciezarek, C. Färber, M. Demmer, F. Dettori, E. Gersabeck, J. Grabowski, W. D. Hulsbergen, B. Khanji, M. Kolpin, M. Kucharczyk, B. P. Malecki, M. Merk, M. Mulder, J. Müller, V. Mueller, A. Pellegrino, M. Pikies, B. Rachwal, T. Schmelzer, B. Spaan, M. Szczekowski, J. Tilburg, S. Tolk, N. Tuning, U. Uwer, J. Wishahi, and M. Witek, J. Inst. **12**, P11016 (2017), arXiv: 1708.00819.

58 M. Adinolfi, G. Aglieri Rinella, E. Albrecht, T. Bellunato, S. Benson, T. Blake, C. Blanks, S. Brisbane, N. H. Brook, M. Calvi, B. Cameron, R. Cardinale, L. Carson, A. Contu, M. Coombes, C. D'Ambrosio, S. Easo, U. Egede, S. Eisenhardt, E. Fanchini, C. Fitzpatrick, F. Fontanelli, R. Forty, C. Frei, P. Gandini, R. Gao, J. Garra Tico, A. Giachero, V. Gibson, C. Gotti, S. Gregson, T. Gys, S. C. Haines, T. Hampson, N. Harnew, D. Hill, P. Hunt, M. John, C. R. Jones, D. Johnson, N. Kanaya, S. Katvars, U. Kerzel, Y. M. Kim, S. Koblitz, M. Kucharczyk, D. Lambert, A. Main, M. Maino, S. Malde, N. Mangiafave, C. Matteuzzi, G. Mini', A. Mollen, J. Morant, R. Mountain, J. V. Morris, F. Muheim, R. Muresan, J. Nardulli, P. Owen, A. Papanestis, M. Patel, G. N. Patrick, D. L. Perego, G. Pessina, A. Petrolini, D. Piedigrossi, R. Plackett, S. Playfer, A. Powell, J. H. Rademacker, S. Ricciardi, G. J. Rogers, P. Sail, M. Sannino, T. Savidge, I. Sepp, S. Sigurdsson, F. J. P. Soler, A. Solomin, F. Soomro, A. Sparkes, P. Spradlin, B. Storaci, C. Thomas, S. Topp-Joergensen, N. Torr, O. Ullaland, K. Vervink, D. Voong, D. Websdale, G. Wilkinson, S. A. Wotton, K. Wyllie, F. Xing, and R. Young, Eur. Phys. J. C **73**, 2431 (2013), arXiv: 1211.6759.

59 R. Aaij, J. Albrecht, F. Alessio, S. Amato, E. Aslanides, I. Belyaev, M. Beuzekom, E. Bonaccorsi, R. Bonnefoy, L. Brarda, O. Callot, M. Cattaneo, H. Chanal, M. Chebbi, X. C. Vidal, M. Clemencic, J. Closier, V. Coco, J. Cogan, O. Deschamps, H. Dijkstra, C. Drancourt, R. Dzhelyadin, M. Frank, M. Gandelman, C. Gaspar, V. V. Gligorov, C. Göbel, L. A. G. Cardoso, Y. Guz, C. Haen, J. He, E. Herwij-

nen, W. Hulsbergen, R. Jacobsson, B. Jost, T. M. Karbach, U. Kerzel, P. Koppenburg, G. Krocker, C. Langenbruch, I. Lax, R. L. Gac, R. Lefévre, J. Lefrançois, O. Leroy, L. L. Gioi, G. Liu, F. Machefert, I. V. Machikhiliyan, M. Magne, G. Mancinelli, U. Marconi, A. M. Sánchez, M. N. Minard, S. Monteil, N. Neufeld, V. Niess, S. Oggero, A. P. C. Yzquierdo, P. Perret, M. Perrin-Terrin, B. Pietrzyk, A. P. Navarro, G. Raven, P. Robbe, H. Ruiz, M. H. Schune, R. Schwemmer, J. Serrano, I. Shapoval, T. Skwarnicki, B. S. D. Paula, P. Spradlin, S. Stahl, V. K. Subbiah, S. T'Jampens, F. Teubert, C. Thomas, M. Vesterinen, M. Williams, M. Witek, and A. Zvyagin, J. Inst. **8**, P04022 (2013), arXiv: 1211.3055.

60 T. Sjöstrand, S. Mrenna, and P. Skands, Comput. Phys. Commun. **178**, 852 (2008), arXiv: 0710.3820.

61 T. Sjöstrand, S. Mrenna, and P. Skands, J. High Energ. Phys. **05**, 026 (2006).

62 I. Belyaev, T. Brambach, N. H. Brook, N. Gauvin, G. Corti, K. Harrison, P. F. Harrison, J. He, C. R. Jones, M. Lieng, G. Manca, S. Miglioranzi, P. Robbe, V. Vagnoni, M. Whitehead, and J. Wishahi, J. Phys.-Conf. Ser. **331**, 032047 (2011).

63 C. H. Chang, J. X. Wang, and X. G. Wu, Comput. Phys. Commun. **181**, 1144 (2010), arXiv: 0910.4462.

64 D. J. Lange, Nucl. Instrum. Meth. Phys. Res. A **462**, 152 (2001).

65 P. Golonka, and Z. Was, Eur. Phys. J. C **45**, 97 (2006).

66 J. Allison, et al. (Geant4 Collaboration), IEEE Trans. Nucl. Sci. **53** 270 (2006).

67 S. Agostinelli, et al. (Geant4 Collaboration), Nucl. Instrum. Meth. Phys. Res. A **506**, 250 (2003).

68 M. Clemencic, G. Corti, S. Easo, C. R. Jones, S. Miglioranzi, M. Pappagallo, and P. Robbe, J. Phys.-Conf. Ser. **331**, 032023 (2011).

69 A. Gulin, I. Kuralenok, and D. Pavlov, in *Winning the transfer learning track of Yahoo!'s learning to rank challenge with YetiRank: Proceedings of the Learning to Rank Challenge*, Proceedings of Machine Learning Research, volume 14, held on 25 June 2010, Haifa, Israel (PMLR, Haifa, 2010), pp. 63-76.

70 T. Likhomanenko, P. Ilten, E. Khairullin, A. Rogozhnikov, A. Ustyuzhanin, and M. Williams, J. Phys.-Conf. Ser. **664**, 082025 (2015), arXiv: 1510.00572.

71 L. Breiman, J. H. Friedman, R. A. Olshen, and C. J. Stone, *Classification and Regression Trees* (Wadsworth International Group, Belmont, 1984).

72 H. Voss, A. Hoecker, J. Stelzer, and F. Tegenfeldt, *TMVA - Toolkit for Multivariate Data Analysis with ROOT: XI International Workshop on Advanced Computing and Analysis Techniques in Physics Research* April 23-27 2007, Amsterdam, the Netherlands (PoS, 2007), PoS (ACAT) 040.

73 A. Hoecker, P. Speckmayer, J. Stelzer, J. Therhaag, E. von Toerne, and H. Voss, *TMVA 4—Toolkit for Multivariate Data Analysis with ROOT*, Users Guide, Technical Report (2009).

74 W. D. Hulsbergen, Nucl. Instrum. Meth. Phys. Res. A **552**, 566 (2005).

75 G. Punzi, *Sensitivity of searches for new signals and its optimization: Statistical Problems in Particle Physics, Astrophysics, and Cosmology, Proceedings of the PHYSTAT 2003 Conference* held 8-11 September, 2003 at the Stanford Linear Accelerator Center (SLAC eConf C030908) (2003).

76 M. Tanabashi, et al. (Particle Data Group), Phys. Rev. D **98**, 030001 (2018).

77 T. Skwarnicki, *A Study of the Radiative Cascade Transitions Between the Upsilon-Prime and Upsilon Resonances*, Dissertation for Doctoral Degree (Institute of Nuclear Physics, Krakow, 1986).

78 S. S. Wilks, Ann. Math. Statist. **9**, 60 (1938).

79 I. Narsky, Nucl. Instrum. Meth. Phys. Res. A **450**, 444 (2000).

80 E. Gross, and O. Vitells, Eur. Phys. J. C **70**, 525 (2010), arXiv: 1005.1891.

81 A. D. Bukin, arXiv: 0711.4449.

82 M. Pivk, and F. R. Le Diberder, Nucl. Instrum. Meth. Phys. Res. A **555**, 356 (2005).

83 R. Aaij, et al. (LHCb Collaboration), J. Inst. **10**, P02007 (2015), arXiv: 1408.1251.

84 L. Anderlini, A. Contu, C. R. Jones, S. S. Malde, D. Muller, S. Ogilvy, J. M. O. Goicochea, A. Pearce, I. Polyakov, W. Qian, B. Sciascia, R. V. Gomez, and Y. Zhang, *The PIDCalib Package*, Technical Report, LHCb-PUB-2016-021 (2016).

85 R. Aaij, L. Anderlini, S. Benson, M. Cattaneo, P. Charpentier, M. Clemencic, A. Falabella, F. Ferrari, M. Fontana, V. V. Gligorov, D. Hill, T. Humair, C. R. Jones, O. Lupton, S. Malde, C. M. Benito, R. Matev, A. Pearce, A. Poluektov, B. Sciascia, F. Stagni, R. V. Gomez, and Y. Zhang, EPJ Tech. Instrum. **6**, 1 (2019).